ADVANCED MATERIALS

Size-Dependent Chemical and Magnetic Ordering in $L1_0$-FePt Nanoparticles**

By *Chuan-bing Rong*, *Daren Li*, *Vikas Nandwana*, *Narayan Poudyal*, *Yong Ding*, *Zhong Lin Wang*, *Hao Zeng*, and *J. Ping Liu**

FePt nanoparticles have great application potential in advanced magnetic materials such as ultrahigh-density recording media and high-performance permanent magnets.[1–3] The key for applications is the very high uniaxial magnetocrystalline anisotropy of the $L1_0$-FePt phase, which is based on crystalline ordering of the face-centered tetragonal (fct) structure, described by the chemical-ordering parameter S.[4] Higher chemical ordering results in higher magnetocrystalline anisotropy. Unfortunately, as-synthesized FePt nanoparticles take a disordered face-centered cubic (fcc) structure that has low magnetocrystalline anisotropy. Heat-treatment is necessary to convert the fcc structure to the ordered fct structure. Several previous theoretical and experimental investigations have been reported on the size-dependent chemical ordering of FePt nanoparticles.[5–9] It has been observed that the degree of ordering decreases with decreasing particle size of the sputtered FePt nanoparticles.[5,6] Theoretical simulation predicted that the ordering would not take place when the particle size is below a critical value.[8,9] However, there have not been systematic experimental studies on quantitative size dependence of chemical ordering of FePt nanoparticles due to the lack of monodisperse $L1_0$-FePt nanoparticles with controllable sizes.

There are also few studies reported to date on the quantitative particle size dependence of magnetic properties, including the Curie temperature, coercivity, and magnetization of the $L1_0$-FePt phase, although it has been well accepted that there is a size effect on the ferromagnetism of any low-dimensional magnets.[10,11] Additionally, the magnetic properties of FePt ferromagnets, as observed in thin-film samples,[4,12] are affected by the degree of chemical ordering, which is in turn size dependent. It is therefore highly desirable to understand the size and chemical-ordering effects, and their influence on the magnetic properties of the nanoparticles.

A major hurdle in obtaining the particle size dependence of structural and magnetic properties of the $L1_0$ phase is particle sintering during heat-treatments that convert the fcc phase to the fct phase.[13,14] This long-pending problem has been solved recently by adopting the salt-matrix annealing technique.[15,16] With this technique, particle aggregation during the phase transformation has been avoided so that the true size-dependent properties of the fct phase can be measured. In this paper, we report results on quantitative particle size dependence of the chemical-ordering parameter S and selected magnetic properties, including the Curie temperature, T_c, magnetization, M_s, and coercivity, H_c, with the particle size varying from 2 to 15 nm.

Figure 1 shows the transmission electron microscopy (TEM) images of the FePt nanoparticles with different sizes before and after annealing in a salt matrix at 973 K for 4 h. The images, from left to right, show nanoparticles with nominal diameters of 2, 4, 6, 8, and 15 nm, respectively. The upper and lower rows are images of as-synthesized and salt-matrix-annealed nanoparticles, respectively. As shown in Figure 1, the particle size is retained well upon annealing. Both the as-synthesized and annealed nanoparticles are monodisperse with a standard deviation of 5–10 % in diameter. TEM observations also revealed that when the particle size is smaller than or equal to 8 nm, the fct nanoparticles are monocrystalline, whereas the 15 nm fct particles are polycrystalline.[15] It is interesting to see that the $L1_0$ nanoparticles, tiny ferromagnets at room temperature, are dispersed very well without agglomeration despite the dipolar interaction between the particles, if a solvent with high viscosity is chosen and if the solution is diluted. Extensive TEM and X-ray diffraction (XRD) analyses have proved that the technique of salt-matrix annealing can be applied to heat-treatments of the FePt nanoparticles without leading to particle agglomeration and sintering, if a suitable salt-to-particle ratio and proper annealing conditions are chosen.[16]

Figure 2 shows the XRD patterns of the 4 nm, as-synthesized, fcc-structured nanoparticles and the particles annealed in a salt matrix at 873 K for 2 h, 973 K for 2 h, and 973 K for 4 h (from bottom to top), respectively. As shown in the figure, the positions of the (111) peaks shift in the higher-an-

[*] Dr. J. P. Liu, Dr. C.-b. Rong, D. Li, V. Nandwana, N. Poudyal
Department of Physics
University of Texas at Arlington
Arlington, TX 76019 (USA)
E-mail: pliu@uta.edu
Dr. Y. Ding, Dr. Z. L. Wang
School of Materials Science and Engineering
Georgia Institute of Technology
Atlanta, GA 30332 (USA)
Dr. H. Zeng
Department of Physics, University at Buffalo
The State University of New York
Buffalo, NY 14260 (USA)
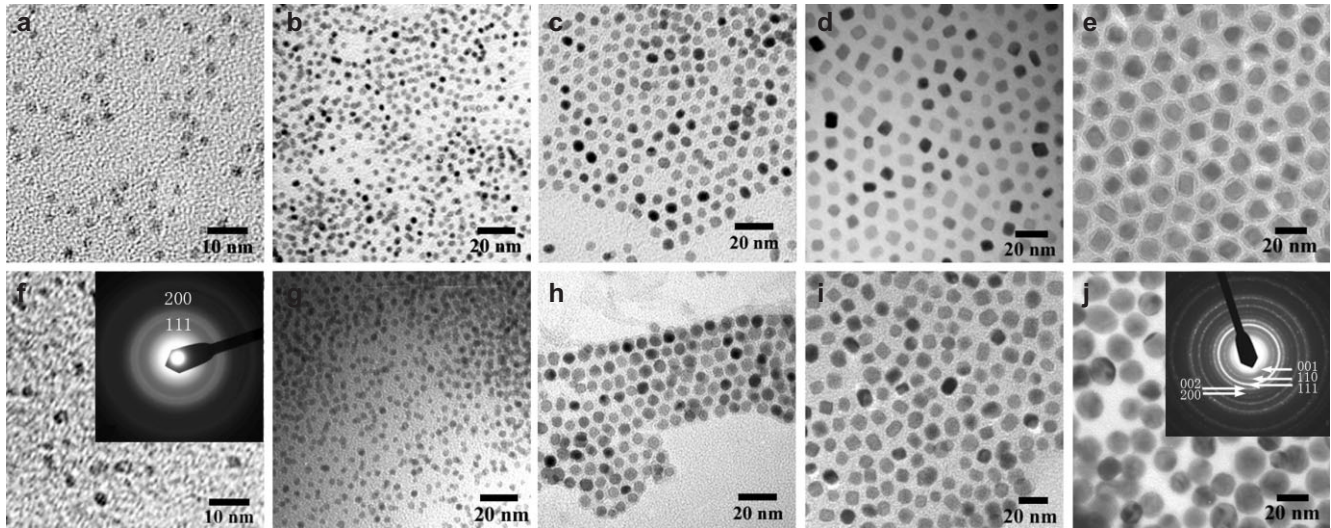
Figure 1. TEM images of as-synthesized FePt nanoparticles of a) 2, b) 4, c) 6, d) 8, and e) 15 nm, and salt-annealed nanoparticles of f) 2, g) 4, h) 6, i) 8, and j) 15 nm. The annealing conditions for a 2 nm particle are 973 K for 8 h, while those for other particles are 973 K for 4 h. The SAED patterns are also given for 2 and 15 nm salt-annealed particles.
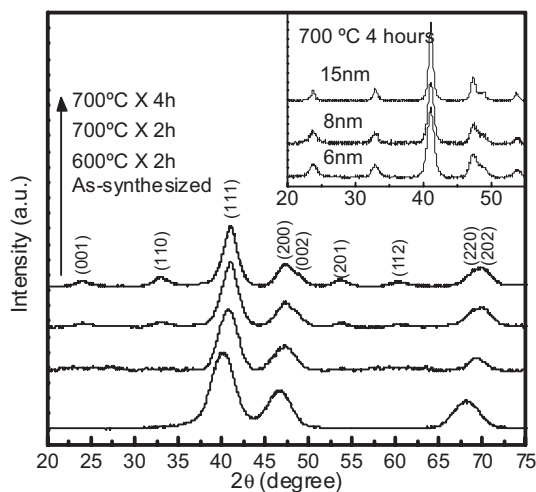
Figure 2. XRD patterns of 4 nm FePt nanoparticles annealed at different parameters. The inset gives the XRD patterns of 6, 8, and 15 nm nanoparticles annealed in salt matrix at 973 K for 4 h.

gle direction with increasing annealing temperature and time. This shift was caused by the change of lattice parameters during the phase transition from fcc to fct. The (001) and (110) peaks, which are the characteristic superlattice peaks of the ordered fct phase, developed with increasing annealing temperature and time. For samples annealed at 973 K for 4 h, the superlattice peaks (001) and (110) were fully developed, implying an fcc–fct transition. The inset of Figure 2 also gives the XRD patterns of the converted fct phase of 6, 8, and 15 nm nanoparticles annealed at 973 K for 4 h in a salt matrix. The grain sizes estimated by the Scherrer formula are about 4.7, 6.8, 8.2, and 13.3 nm for the 4, 6, 8, and 15 nm nanoparticles, respectively, which matches the particle sizes

very well. The relatively smaller grain size of the 15 nm nanoparticles is due to the polycrystalline morphology mentioned above.

XRD does not give any diffraction peaks for the 2 nm FePt particles, largely because of the lower crystallinity, strong surface effects, and/or peak broadening due to the small size. Selected area electron diffraction (SAED) was therefore also used to identify the crystalline structure of the particles, especially for the smaller particles. The SAED patterns showed that the annealed nanoparticles are $L1_0$-fct phase if the particle size is equal to or larger than 4 nm. However, the SAED pattern of 2 nm particles, which is given in the inset of Figure 1f, does not show (001) and (110) rings (in contrast to the SAED pattern of the fct nanoparticles shown in Fig. 1j). This indicates that the 2 nm FePt particles cannot be transformed to the $L1_0$-fct structure. We extended the annealing time to 8 h and the results remained the same. This direct experimental observation is consistent with the theoretical predictions and is fundamentally important as well as being significant for specific applications.[8,9] It can be concluded that when the particle size is smaller than a critical value of around 3 nm, chemical ordering will not take place.

To evaluate the effect of chemical ordering of the $L1_0$ phase in a quantitative way, the following equation was used to calculate the ordering parameter S[17–19]

$$S \cong 0.85 \left[\frac{I_{001}}{I_{002}} \right]^{1/2} \tag{1}$$

where I_{001} and I_{002} are the integrated intensities of the (001) and (002) diffraction peaks from the XRD patterns. The long-range S value of fct-FePt nanoparticles with different sizes, annealed under the same conditions (973 K, 4 h), was calcu-

lated according to Equation 1. Figure 3 shows the correlation between S and particle size. Each experimental point was obtained by measuring at least four different samples and the error bar is the standard deviation. As expected, S decreases with reducing particle size. In the case of 2 nm FePt particles, S vanishes because no superlattice structure can be found.
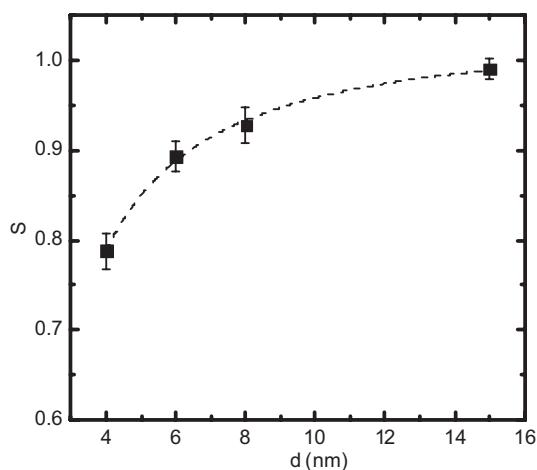
Figure 3. The dependence of the long-range ordering parameter on particle size. The dashed line is a guide to the eye.

Figure 4 shows the hysteresis loops at 300 K of the fct nanoparticles with different sizes. It shows that the coercivity, H_c, increases with increasing particle size (d) as $d \leq 8$ nm. Giant coercivity values of up to 30 kOe (1 Oe = 79.57 A m^{-1}) have been achieved from the monodisperse hard magnetic nanoparticles, which give the particles great potential for applications. The enhancement of H_c with increased particle size can be attributed partly to the size-dependent chemical ordering discussed above. However, larger particles of 15 nm have lower H_c than the 8 nm particles. This may be caused by the polycrystalline structure, as intergranular exchange coupling
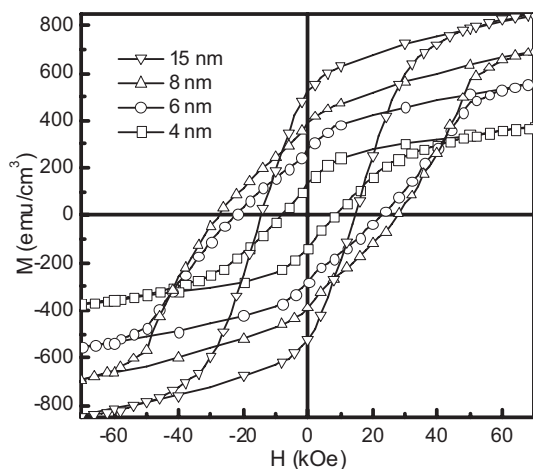
**Figure 4.** Hysteresis loops of salt-annealed 4, 6, 8, and 15 nm nanoparticles.

leads to reduced magnetocrystalline anisotropy.[20] The exchange coupling can be further seen from the relatively high remanence ratio $M_r/M_s > 0.5$, where M_r and M_s are remanence and saturation magnetization, respectively (we used the magnetization values at 7 T as an approximation of M_s). The reduced coercivity may also be attributed to multiple c-axes within a nanoparticle, which can lead to a significantly reduced effective anisotropy.[21]

Figure 4 shows that the M_s values decrease with decreasing particle size and are lower than the value for the bulk $L1_0$ phase (1140 emu cm^{-3} (1 emu cm^{-3} = 1000 A m^{-3}) at room temperature).[22] Figure 5 gives M_s at 300 K plotted against $1/d$. A linear correlation was obtained. However, the linearly extrapolated M_s is lower than the experimental value since the hysteresis curve in this work is not saturated for the applied field of 70 kOe. The main reason for this linear reduction may be related to the reduced magnetization on the surfaces of the nanoparticles.[23–25]
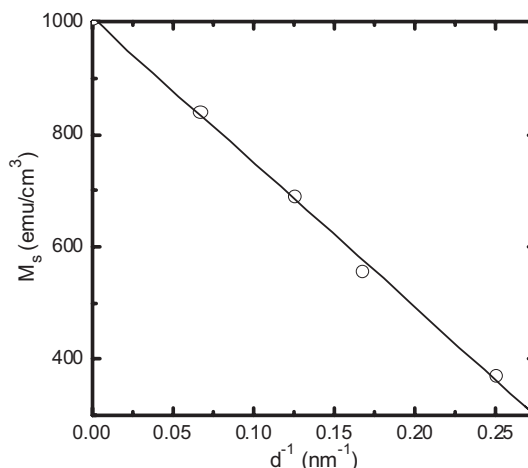
Figure 5. The relation between M_s and particle size.

It is of fundamental interest to understand the correlation between particle size and Curie temperature of high-anisotropy nanoparticles. Most studies on low-dimensional ferromagnets reported so far are on granular thin films and nanocomposites where grain polydispersity and existence of matrix materials mask the genuine size effect.[26] The magnetic-ordering temperatures of ferromagnets with reduced size in all three dimensions have been little studied because of a lack of monodisperse, ferromagnetic nanoparticles with small sizes. This challenge has been addressed by applying the salt-matrix-annealing technique, with which ferromagnetic nanoparticles with high anisotropy at room temperature are obtained. Figure 6 shows the dependence of the Curie temperature on the fct-FePt particle size (open squares). It should be noted that S for these points corresponds to the values in Figure 3. We measured the magnetization M versus T in an applied field of 1 kOe. Each point was obtained by averaging data from at least four different samples with two M–T measure-
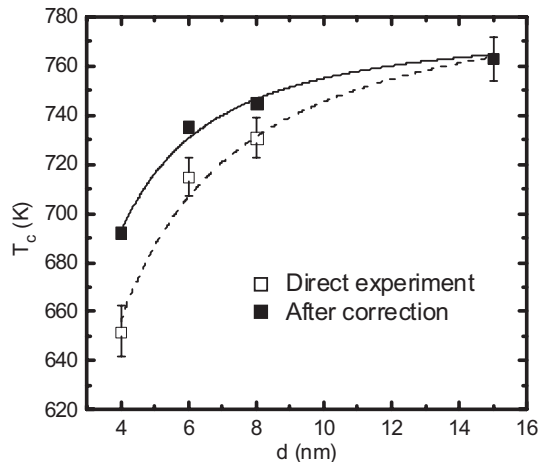
Figure 6. The dependence of Curie temperature on the particle size. The dashed line is a guide to the eye and the solid lines are made by fitting the data.

ments for each sample. The error bar is based on the statistical standard deviation. To prevent sintering and agglomeration of the particles during the measurements, we kept the nanoparticles in the salt matrix. T_c was determined from the intersection of extrapolations of the greatest slope and flat region above T_c. As shown in Figure 6, T_c decreases remarkably with declining particle size, especially when $d < 6$ nm. For the 2 nm nanoparticles, we could not obtain T_c for the fct phase since the phase transition cannot be realized.

To understand the strong size dependence of the Curie temperature, the finite-size-scaling theory was used to fit the behavior of T_c.[10,11] This theory predicts that the shift of T_c from the value for bulk materials depends on the dimension in the following manner

$$\frac{T_c(\infty) - T_c(d)}{T_c(\infty)} = \left(\frac{d}{d_0}\right)^{-1/\nu} \qquad (2)$$

where $T_c(d)$ is the Curie temperature as a function of d, $T_c(\infty)$ is the bulk Curie temperature, d_0 is a constant, and ν is the critical exponent of the correlation length. By fitting the data in Figure 6 (the open squares), $T_c(\infty) = (795 \pm 10)$ K, $d_0 = (0.84 \pm 0.05)$ nm, and $\nu = (0.91 \pm 0.10)$ were obtained. The value of d_0, which is comparable to the lattice constant, and is the microscopic length scale, is reasonable. However, the fitting value of ν is out of the range $\nu = (0.65 \pm 0.07)$ to (0.73 ± 0.02) predicted by the isotropic three-dimensional Heisenberg model.[27] In addition, $T_c(\infty)$ is remarkably higher than the known T_c of bulk FePt materials.[22,27] The discrepancies may be due to the influence of chemical ordering on the Curie temperature.

To distinguish the effects of particle size and chemical ordering on the Curie temperature, we performed T_c measurements with fixed particle size of 8 nm. Samples with a series of ordering parameters were obtained by adjusting the salt-

matrix-annealing time and temperature. Figure 7 gives the dependence of the Curie temperature on the ordering parameters of the 8 nm particles. It shows that T_c increases linearly with increasing S. The data can be fitted well in the region $0.6 \leq S \leq 1.0$ by a linear relation $T_c = T_{c0} + aS$, where $T_{c0} = (570 \pm 18)$ K and $a = (190 \pm 20)$ K are fitting parameters.
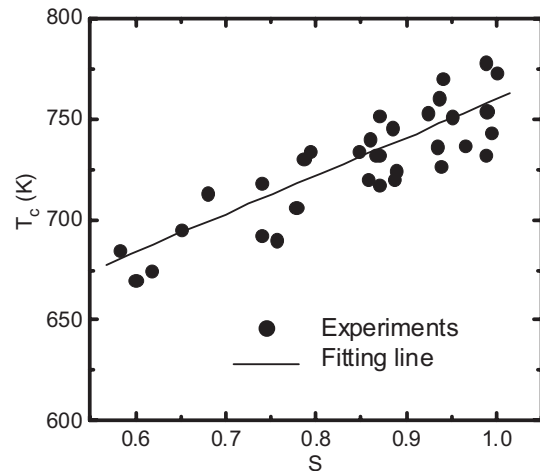
Figure 7. The correlation between the ordering parameters and the Curie temperature with fixed particle size of 8 nm.

This linear correlation has also been obtained for the fct particles of 4 nm. It is striking to see such strong correlation between the magnetic-ordering temperature and the chemical-ordering parameter. Previous studies based on sputtered thin films showed that the disordered fcc-FePt phase has a T_c lower than that of the ordered fct-FePt phase but with a weak dependence on the ordering.[12,28] Further work is needed to fully understand the strong correlation in the nanoparticles.

By correcting for the ordering effect, we can obtain the real particle size effect on the Curie temperature of fully ordered fct-FePt nanoparticles, as represented by the solid squares in Figure 6. The best fits of the data give $T_c(\infty) = (775 \pm 20)$ K, $\nu = (0.67 \pm 0.11)$, and $d_0 = (0.90 \pm 0.10)$ nm. The fitted value of ν is consistent with the known value of ν for magnetic systems, which is in the range (0.65 ± 0.07).[27] The fitted value of d_0 is a little more than twice the unit-cell size and is reasonable. The fitted value of $T_c(\infty)$ of (775 ± 20) K is slightly higher than the reported 750 K for bulk fct-FePt material but the deviation is comparable to the experimental error. The Fe-rich composition could contribute to this deviation. Thus, the dependence of the Curie temperature on the particle size is generally consistent with finite-size-scaling theory. Although in such a model only nearest-neighbor interactions are considered, in FePt systems both long-range exchange interactions and exchange mediated by Pt should be taken into account. Modeling efforts including these longer-range interactions and the surface effect are underway.

In summary, we have studied the size dependence of the chemical-ordering parameter and magnetic-ordering proper-

ties including coercivity, magnetization, and Curie temperature of fct-FePt nanoparticles. Based on the newly developed salt-matrix-annealing technique, direct experimental evidence has been found that the long-range ordering parameter S decreases with decreasing particle size d. The chemical ordering does not occur for $d \leq 2$ nm. It is also revealed that magnetic properties including Curie temperature, magnetization, and coercivity are strongly dependent on both the particle size and the chemical ordering. The interplay between the size effect and the chemical-ordering effect defines the magnetic behavior. The shift in T_c can generally be described by the finite-size-scaling theory after considering the chemical-ordering effect on T_c.

Experimental

The fcc-structured FePt nanoparticles with different sizes (from 2 to 15 nm) were synthesized using a chemical-solution method with adjusted synthetic parameters.[1,29,30] The fcc particles were then mixed with ball-milled NaCl powder in hexane or another organic solvent with the assistance of surfactants. Dry mixtures of FePt particles and NaCl powders were obtained after the solvent was evaporated completely. The mixtures were then annealed in a forming gas (93% Ar+7% H$_2$) at different temperatures for different times. After the annealing, the NaCl powder was washed away by deionized water and the FePt nanoparticles were recovered and dispersed in organic solvents, such as cyclohexane or ethanol, in the presence of surfactants. The elemental composition analyses, using inductively coupled plasma-optical emission spectroscopy (ICP-OES), showed that there was negligible NaCl contamination in the salt-matrix-annealed FePt nanoparticles and the particle composition was Fe$_{52}$Pt$_{48}$. A transmission electron microscope was used to analyze the morphology and crystalline structures. X-ray diffraction (XRD) was used to determine the phase transition, the long-range ordering parameters, the grain size, and the particle size. The magnetic hysteresis loops were measured with a magnetic properties measurement system (MPMS) from specimens of a mixture of epoxy and the magnetic nanoparticles. Curie temperatures were measured by a physical properties measurement system (PPMS) with high-temperature and high-vacuum vibrating sample magnetometer.

[1] S. H. Sun, C. B. Murray, D. Weller, L. Folks, A. Moser, *Science* **2000**, *287*, 1989.

[2] H. Zeng, J. Li, J. P. Liu, Z. L. Wang, S. H. Sun, *Nature* **2002**, *420*, 395.

[3] C. B. Rong, H. W. Zhang, X. B. Du, J. Zhang, S. Y. Zhang, B. G. Shen, *J. Appl. Phys.* **2004**, *96*, 3921.

[4] R. A. Ristau, K. Barmak, L. H. Lewis, K. R. Coffey, J. K. Howard, *J. Appl. Phys.* **1999**, *86*, 4527.

[5] Y. K. Takahashi, T. Ohkubo, M. Ohnuma, K. Hono, *J. Appl. Phys.* **2003**, *93*, 7166.

[6] T. Miyazaki, O. Kitakami, S. Okamoto, Y. Shimada, Z. Akase, Y. Murakami, D. Shindo, Y. K. Takahashi, K. Hono, *Phys. Rev. B: Condens. Matter Mater. Phys.* **2005**, *72*, 144 419.

[7] Z. Y. Jia, S. S. Kang, S. F. Shi, D. E. Nikles, J. W. Harrell, *J. Appl. Phys.* **2005**, *97*, 10J 310.

[8] R. V. Chepulskii, W. H. Butler, *Phys. Rev. B: Condens. Matter Mater. Phys.* **2005**, *72*, 134 205.

[9] B. Yang, M. Asta, O. N. Mryasov, T. J. Klemmer, R. W. Chantrell, *Scr. Mater.* **2005**, *53*, 417.

[10] K. Binder, *Physica* **1972**, *62*, 508.

[11] M. Farle, K. Baberschke, U. Stetter, A. Aspelmeier, F. Gerhardter, *Phys. Rev.* **1993**, *47*, 11 571.

[12] S. Okamoto, N. Kikuchi, O. Kitakami, T. Miyazaki, Y. Shimada, K. Fukamichi, *Phys. Rev. B: Condens. Matter Mater. Phys.* **2002**, *66*, 024 413.

[13] H. Zeng, S. H. Sun, T. S. Vedantam, J. P. Liu, Z. R. Dai, Z. L. Wang, *Appl. Phys. Lett.* **2002**, *80*, 2583.

[14] T. Thomson, S. L. Lee, M. F. Toney, C. D. Dewhurst, F. Y. Ogrin, C. J. Oates, S. Sun, *Phys. Rev. B: Condens. Matter Mater. Phys.* **2005**, *72*, 064 441.

[15] K. Elkins, D. Li, N. Poudyal, V. Nandwana, Z. Jin, K. Chen, J. P. Liu, *J. Phys. D: Appl. Phys.* **2005**, *38*, 2306.

[16] D. Li, N. Poudyal, V. Nandwana, Z. Jin, K. Elkins, J. P. Liu, *J. Appl. Phys.* **2006**, *99*, 08E 911.

[17] B. E. Warren, *X-Ray Diffraction*, Dover Publications, New York **1990**, Ch. 12.

[18] A. Cebollada, D. Weller, J. Sticht, G. R. Harp, R. F. C. Farrow, R. F. Marks, R. Savoy, J. C. Scott, *Phys. Rev. B: Condens. Matter Mater. Phys.* **1994**, *50*, 3419.

[19] J. A. Christodoulides, P. Farber, M. Daniil, H. Okumura, G. C. Hadjipanayis, V. Skumryev, A. Simopoulos, D. Weller, *IEEE Trans. Magn.* **2001**, *37*, 1292.

[20] G. Herzer, *IEEE Trans. Magn.* **1989**, *25*, 3327.

[21] W. Scholz, J. Fidler, T. Schrefl, D. Suess, H. Forster, R. Dittrich, V. Tsiantos, *J. Magn. Magn. Mater.* **2004**, *272-276*, 1524.

[22] T. Klemmer, D. Hoydick, H. Okumura, B. Zhang, W. A. Soffa, *Scr. Metall. Mater.* **1995**, *33*, 1793.

[23] A. E. Berkowitz, W. J. Schuele, P. J. Flanders, *J. Appl. Phys.* **1987**, *39*, 1261.

[24] Z. X. Tang, C. M. Sorensen, K. J. Klabunde, G. C. Hadjipanayis, *Phys. Rev. Lett.* **1991**, *67*, 3602.

[25] J. P. Chen, C. M. Sorensen, K. J. Klabunde, G. C. Hadjipanayis, *Phys. Rev. B: Condens. Matter Mater. Phys.* **1996**, *54*, 9288.

[26] H. Zeng, R. Sabirianov, O. Mryasov, M. L. Yan, K. Cho, D. J. Sellmyer, *Phys. Rev. B: Condens. Matter Mater. Phys.* **2002**, *66*, 184 425.

[27] S. N. Kaul, *J. Magn. Magn. Mater.* **1985**, *53*, 5.

[28] M. Watanabe, T. Nakayama, K. Watanabe, T. Hirayama, A. Tonomura, *Mater. Trans., JIM* **1996**, *37*, 489.

[29] K. E. Elkins, T. S. Vedantam, J. P. Liu, H. Zeng, S. Sun, Y. Ding, Z. L. Wang, *Nano Lett.* **2003**, *3*, 1647.

[30] M. Chen, J. P. Liu, S. Sun, *J. Am. Chem. Soc.* **2004**, *126*, 8394.